

Accurate and efficient gravitational waveforms for certain galactic compact binaries

Manuel Tessmer ^{*} and Achamveedu Gopakumar [†]

Theoretisch-Physikalisches Institut, Friedrich-Schiller-Universität, Max-Wien-Platz 1, 07743 Jena, Germany

10 September 2018

ABSTRACT

Stellar-mass compact binaries in eccentric orbits are almost guaranteed sources of gravitational waves for Laser Interferometer Space Antenna. We present a prescription to compute accurate and efficient gravitational-wave polarizations associated with bound compact binaries of arbitrary eccentricity and mass ratio moving in slowly precessing orbits. We compare our approach with those existing in the literature and present its advantages.

Key words: gravitational waves – methods: compact binaries: general.

1 INTRODUCTION

It is expected that the Laser Interferometer Space Antenna (LISA) will usher in a new era for gravitational-wave (GW) astronomy. The galactic stellar-mass compact binaries are highly promising sources for LISA. These are also excellent sources to do astrophysics with LISA, which requires accurate extraction of astrophysical informations from gravitational waves they emit; the real goal of GW astronomy. Accurate extraction of astrophysical quantities associated with compact binaries is possible, in principle, as the dynamics of these sources, when gravitational waves they emit enter LISA’s bandwidth, is very accurately described by the post-Newtonian (PN) approximation to general relativity. The PN approximation allows one to express the equations of motion of a compact binary as corrections to the Newtonian equations of motion in powers of $(v/c)^2 \sim Gm/(c^2R)$, where v , m and R are the characteristic orbital velocity, the total mass, and the typical orbital separation of the binary, respectively.

An important feature of stellar-mass compact binaries, relevant for LISA, consisting of neutron stars, stellar-mass black holes or a mixture of both may be that they will have non-negligible eccentricities, as demonstrated by several astrophysically motivated investigations (Benacquista 2002; Gusev et al. 2002; Chaurasia & Bailes 2005). Let us first consider a recent investigation that clearly demonstrated that a natural consequence of an asymmetric kick imparted to neutron stars at birth is that the majority of neutron-star (NS) binaries should possess highly eccentric orbits (Chaurasia & Bailes 2005). Chaurasia & Bailes (2005) also

pointed out that their conclusions are applicable to black-hole–neutron-star (BH–NS) and black-hole–black-hole (BH–BH) binaries. Further, the observed deficit of eccentric short period binary pulsars was attributed to selection effects, in pulsar surveys, mainly due to the accelerated decay of these binaries (Chaurasia & Bailes 2005). In another investigation, assuming a stationary distribution for NS–NS binaries in the galaxy, it was argued that LISA will see several NS–NS, NS–BH and BH–BH binaries in eccentric orbits (Gusev et al. 2002). In another investigation that employed Monte Carlo simulations to model galactic globular clusters, it was observed that LISA may see several stellar-mass BH binaries in highly eccentric orbits (Benacquista 2002). Therefore, it is desirable to have accurate and efficient GW templates for stellar-mass compact binaries in eccentric orbits. This is because LISA observations of such compact binaries should provide at least the total mass of these binaries (Seto 2001), angular resolution sufficient to identify their location (Benacquista 2002) and, in principle, a bound for the mass of gravitons (Jones 2005).

In this paper, we provide accurate and efficient GW polarizations which are restricted to the quadrupolar order, $h_{+|Q}$ and $h_{\times|Q}$, associated with compact binaries, modeled to consist of non-spinning point masses, moving in precessing eccentric orbits. These templates, which should be useful for LISA, are accurate as we employ the fully 1PN accurate orbital motion. They are efficient as we provide efficient numerical prescriptions to obtain both time and frequency domain representations for the relevant h_{+} and h_{\times} . We restricted the orbital motion to be fully 1PN accurate and neglected higher PN contributions for the following two reasons. The first one is that the investigations, (Moreno-Garrido et al. 1995; Pierro et al. 2001), that we want to improve (both in accuracy and

^{*} E-mail: m.tessmer@uni-jena.de

[†] E-mail: a.gopakumar@uni-jena.de

efficiency) do not (and can not) even treat the orbital motion in a fully 1PN accurate manner. The second reason is that for stellar-mass compact binaries in eccentric orbits, whose orbital frequency is $\sim 10^{-3}$ Hz, it is more important to include the frequency shift due to the periastron advance (which appears at the 1PN order) compared to the shift caused by the radiation reaction, appearing at the 2.5PN order (Seto 2001). Moreover, the methods we introduce here to construct numerically efficient templates can be, in principle, incorporated into the phasing formalism that gave h_+ and h_\times with fully 3.5PN accurate orbital motion (Damour et al. 2004; Königsdörffer & Gopakumar 2006).

The paper is organized in the following way. In Section 2, we introduce relevant expressions for the 1PN accurate orbital dynamics and the associated h_+ and h_\times , required to construct the templates. Sections 3 and 4 deal with accurate and efficient ways of obtaining the time and frequency domain GW templates. The pictorial depictions of our results and associated detailed discussions are given in Section 5, followed by a brief summary.

2 PN ACCURATE INPUTS FOR TEMPLATES

The two independent GW polarizations for non-spinning compact binaries moving in non-circular orbits, due to the dominant quadrupolar contributions, available in Damour et al. (2004), read

$$h_{\times|Q}(r, \phi, \dot{r}, \dot{\phi}) = -2 \frac{Gm\eta C}{c^4 R'} \left\{ \left(\frac{Gm}{r} + r^2 \dot{\phi}^2 - \dot{r}^2 \right) \sin 2\phi - 2r\dot{r}\dot{\phi} \cos 2\phi \right\}, \quad (1a)$$

$$h_{+|Q}(r, \phi, \dot{r}, \dot{\phi}) = -\frac{Gm\eta}{c^4 R'} \left\{ (1 + C^2) \left[\left(\frac{Gm}{r} + r^2 \dot{\phi}^2 - \dot{r}^2 \right) \times \cos 2\phi + 2r\dot{r}\dot{\phi} \sin 2\phi \right] + S^2 \left(\frac{Gm}{r} - r^2 \dot{\phi}^2 - \dot{r}^2 \right) \right\}. \quad (1b)$$

In these expressions, the symmetric mass ratio $\eta = m_1 m_2 / m^2$, m_1 and m_2 are the individual masses with $m = m_1 + m_2$, R' is the radial distance to the binary and S and C stand for $\cos i$ and $\sin i$, respectively, i being the orbital inclination. The dynamic variables r and ϕ denote the relative separation and the orbital phase of the binary in a suitably defined center of mass frame, with $\dot{r} = \frac{dr}{dt}$ and $\dot{\phi} = \frac{d\phi}{dt}$ [see Damour et al. (2004) for our convention]. In order to obtain a prescription that models the temporal evolutions for $h_{+|Q}$ and $h_{\times|Q}$, namely the GW phasing, we invoke the following parametric descriptions, involving the eccentric anomaly u , for the dynamical variables present in Eqs. (1).

$$r = \left(\frac{Gm}{n^2} \right)^{1/3} (1 - e_t \cos u) \left\{ 1 + \frac{\xi^{2/3}}{6(1 - e_t \cos u)} [-18 + 2\eta - (6 - 7\eta)e_t \cos u] \right\}, \quad (2a)$$

$$\dot{r} = \frac{e_t (Gmn)^{1/3}}{6(1 - e_t \cos u)} \left[6 + \xi^{2/3} (6 - 7\eta) \right] \sin u, \quad (2b)$$

where n is the 1PN accurate mean motion, defined by $n = 2\pi/P$, P being the orbital period, and e_t is the eccentricity associated with the 1PN accurate Kepler equation (KE) displayed below, and ξ stands for Gmn/c^3 . The angular motion, defined by ϕ and $\dot{\phi}$, is given by

$$\phi(\lambda, l) = \lambda + W(l), \quad (3a)$$

$$\lambda = (1 + k)n(t - t_0) + \phi_0, \quad (3b)$$

where t_0 and ϕ_0 are some initial time and associated orbital phase, respectively. The expressions for W and k are given by

$$W(l) = (v - u + e_t \sin u) \left(1 + \frac{3\xi^{2/3}}{1 - e_t^2} \right), \quad (3c)$$

$$k = \frac{3\xi^{2/3}}{1 - e_t^2}, \quad (3d)$$

$$v = 2 \arctan \left[\left(\frac{1 + e_\phi}{1 - e_\phi} \right)^{1/2} \tan \frac{u}{2} \right], \quad (3e)$$

where

$$e_\phi = e_t \left[1 + \xi^{2/3} (4 - \eta) \right]. \quad (3f)$$

The first time derivative of ϕ reads

$$\dot{\phi} = \frac{n\sqrt{1 - e_t^2}}{(1 - e_t \cos u)^2} \left\{ 1 + \frac{\xi^{2/3}}{(1 - e_t^2)(1 - e_t \cos u)} \times \left[3 - (4 - \eta)e_t^2 + (1 - \eta)e_t \cos u \right] \right\}. \quad (3g)$$

We note that derivations of these expressions, available in Damour et al. (2004), require the 1PN accurate quasi-Keplerian parameterization for compact binaries in eccentric orbits (Damour & Deruelle 1985). The explicit time evolution for $h_{+|Q}$ and $h_{\times|Q}$ is achieved by solving the 1PN accurate KE, present in the 1PN accurate quasi-Keplerian parameterization, which reads

$$l \equiv n(t - t_0) = u - e_t \sin u, \quad (4)$$

where l is the mean anomaly. Note that Eq. (4) is structurally identical to the classical (Newtonian accurate) KE, only if we express the PN accurate dynamics in terms of e_t , one of the three eccentricities that appear in the 1PN accurate quasi-Keplerian parameterization. This allows us to adapt the most efficient and accurate (numerical) way of solving the classical KE (Mikkola 1987). We introduce Mikkola's solution in the next section.

3 MIKKOLA'S SOLUTION TO THE RELEVANT KEPLER EQUATION

The celebrated KE has enticed several generations of distinguished scientists roughly from 1650 onward and, therefore, a plethora of solutions exists [see Colwell (1993) for a detailed review]. Even though with the help of fast computers it is easy to obtain accurate and quick solutions to the KE, there exist subtle points associated with the accuracies and efficiencies of various numerical solutions. A numerical solution to the KE usually employs Newton's method which requires an initial guess u_0 that depends on l and e_t . A number of iterations will be required to obtain an approximate

solution that has some desired accuracy. The number of iterations to reach this accuracy naturally depends on u_0 , e_t and l . It is therefore compelling to ask, as done for the first time by E. Schubert in 1854, if there exists a clever choice for u_0 , such that with one iteration of Newton's method one would achieve the desired accuracy for all e_t and l .¹ In 1987, Seppo Mikkola devised a clever empirical procedure which gives u with a relative error $\sim 10^{-15}$, that may be treated to be one of the closest solutions to the puzzle posed by Schubert. In this paper, we employ Mikkola's simple and robust solution to solve the 1PN accurate KE and, therefore, obtain $h_{+|Q}(t)$ and $h_{\times|Q}(t)$ with 1PN accurate orbital evolution. As Mikkola's solution is crucial to obtain highly efficient 1PN accurate phasing, let us briefly describe below Mikkola's procedure.

In order to obtain an efficient prescription for u_0 (an initial guess for u), Mikkola introduced an auxiliary variable $s = \sin(u/3)$, allowing one to write our KE as

$$3 \arcsin s - e_t (3s - 4s^3) = l. \quad (5)$$

Truncating $\arcsin s$ to the third order leads to the following approximate KE

$$3(1 - e_t)s + (4e_t + \frac{1}{2})s^3 = l. \quad (6)$$

The solution to the above cubic equation in s can be expressed as

$$s = z - \frac{\alpha}{z}, \quad (7)$$

where

$$\alpha = \frac{1 - e_t}{4e_t + \frac{1}{2}}, \quad (8a)$$

$$z = \left(\beta \pm \sqrt{\beta^2 + \alpha^3} \right)^{1/3}, \quad (8b)$$

$$(8c)$$

β being

$$\beta = \frac{\frac{1}{2}l}{4e_t + \frac{1}{2}}, \quad (8d)$$

and the sign of the square root is to be chosen to be that of l . Mikkola negated the largest error, occurring at $l = \pi$, by a simple correction term $ds = -0.078 s^5 / (1 + e_t)$. With the help of Eq. (6), the initial guess for u , namely u_0 , becomes

$$u_0 = l + e_t (3\omega - 4\omega^3), \quad (9)$$

where $\omega = s + ds = s - 0.078 s^5 / (1 + e_t)$. It is important to note that u_0 , which enjoys maximum relative error that is not greater than 2×10^{-3} , is obtained without employing a single evaluation of trigonometric functions. Following Mikkola, our transcendental equation, namely the 1PN accurate KE, also requires evaluation of just one square root and one cubic root for its solution. To improve u_0 , one needs to apply a fourth-order extension of Newton's method, available in Danby & Burkardt (1983). This requires us to define $f(u) = u - e_t \sin u - l$ and its first four derivatives with respect to u , evaluated at $u = u_0$. This leads to a solution

to our KE that has a relative error not greater than 10^{-15} , which reads

$$u = u_0 + u_4, \quad (10)$$

where

$$u_1 = -\frac{f}{f'}, \quad (11a)$$

$$u_2 = -\frac{f}{f' + \frac{1}{2}f''u_1}, \quad (11b)$$

$$u_3 = -\frac{f}{f' + \frac{1}{2}f''u_2 + \frac{1}{6}f'''u_2^2}, \quad (11c)$$

$$u_4 = -\frac{f}{f' + \frac{1}{2}f''u_3 + \frac{1}{6}f'''u_3^2 + \frac{1}{24}f''''u_3^3} \quad (11d)$$

It is important to note that the method requires reduction of l into the interval $-\pi \leq l \leq \pi$ in order to make s as small as possible. We employ geometrical interpretations of u and l , and results from Danby & Burkardt (1983), to map any l into the above interval. First consider the case where $l < 0$. We then define $l^* = -l$ and solve $u^* - e_t \sin u^* - l^* = 0$ for u^* and naturally $u = -u^*$. If l is such that $\pi < l < 2\pi$, then there exists $u(l) = 2\pi - u(2\pi - l)$, which follows from the geometrical construction of u and l . If $l > 2\pi$, the situation is subtle and we define $l^* = l - \lfloor \frac{l}{2\pi} \rfloor 2\pi$, where $\lfloor \frac{l}{2\pi} \rfloor$ denotes the integer part of $l/2\pi$, so that l^* lies in the interval $[0, 2\pi]$. This leads to $u(l) = \lfloor \frac{l}{2\pi} \rfloor 2\pi + u^*(l^*)$, which is based on the fact that at the fixed points of KE, $u = l$.

Let us now point out another way of tackling the largest error associated with $l = \pi$, without resorting to the introduction of ds .² The idea is to choose the coefficient of s^3 in the Taylor expansion for $\arcsin s$, such that Eqs. (5) and (6) become identical at $l = \pi$. This can be achieved by replacing $1/6$, the coefficient of s^3 in the Taylor expansion, by $1/(6 + \gamma l)$. It is then straightforward to deduce that $\gamma = -(3/4\pi)(27\sqrt{3} - 16\pi)/(3\sqrt{3} - 2\pi)$ at $l = \pi$. This approach provides u_0 with a relative accuracy $\sim 10^{-3}$ for all e_t and as expected, there is no need to introduce ds .

It is important to realize that Mikkola's solution only demands the solution of a cubic polynomial that involves no trigonometric functions and one-time evaluation of $\sin \omega$ and $\cos \omega$. Further, it applies to all e_t and l with $0 \leq e_t \leq 1$. With the help of Mikkola's solution to 1PN accurate KE, Eq. (4), and employing Eqs. (1), we obtained accurate and efficient temporal evolution for $h_{+|Q}$ and $h_{\times|Q}$. In the next section, we present a way of expressing $h_{+|Q}(t)$ and $h_{\times|Q}(t)$ that easily reveals their spectral contents.

4 FOURIER SERIES REPRESENTATION FOR $H_{\times|Q}$ AND $H_{+|Q}$

In this section, we present a Fourier series expansion of $h_{\times|Q}(t)$ and $h_{+|Q}(t)$, that easily allows one to compute the associated power spectrum. This section is influenced by Section. III of Gopakumar & Iyer (2002) [However, we correct few shortcomings present in that section]. We begin by

¹ See page 98, Colwell (1993)

² We thank Seppo Mikkola for pointing out this (unpublished) esthetically and numerically better prescription for u_0 .

rewriting Eqs. (1) as

$$h_{\times|Q}(t) = \frac{Gm\eta}{c^2 R'} H_{\times|Q}(t), \quad (12a)$$

$$h_{+|Q}(t) = \frac{Gm\eta}{c^2 R'} H_{+|Q}(t), \quad (12b)$$

where $H_{\times|Q}$ and $H_{+|Q}$ symbolically read

$$H_{\times|Q}(t) = X_{2C}(l) \cos 2\lambda + X_{2S}(l) \sin 2\lambda, \quad (13a)$$

$$H_{+|Q}(t) = P_{2C}(l) \cos 2\lambda + P_{2S}(l) \sin 2\lambda + P_0(l). \quad (13b)$$

We note that $X_{2C}(l)$, $X_{2S}(l)$, $P_{2C}(l)$, $P_{2S}(l)$ and $P_0(l)$ are 2π -periodic implicit functions of l (and explicit functions of u) and can be obtained with the help of Eqs. (1) after using the $\phi = \lambda + W$ split. Their exact expressions, in terms of the dynamical variables, are given by

$$X_{2C}(l) = -\frac{2C}{c^2} \left\{ \left(\frac{Gm}{r} + \dot{\phi}^2 r^2 - \dot{r}^2 \right) \sin 2W - 2r\dot{r}\dot{\phi} \cos 2W \right\}, \quad (14a)$$

$$X_{2S}(l) = -\frac{2C}{c^2} \left\{ \left(\frac{Gm}{r} + \dot{\phi}^2 r^2 - \dot{r}^2 \right) \cos 2W + 2r\dot{r}\dot{\phi} \sin 2W \right\}, \quad (14b)$$

$$P_{2C}(l) = -\frac{(1+C^2)}{c^2} \left\{ \left(\frac{Gm}{r} + \dot{\phi}^2 r^2 - \dot{r}^2 \right) \cos 2W + 2r\dot{r}\dot{\phi} \sin 2W \right\}, \quad (14c)$$

$$P_{2S}(l) = \frac{(1+C^2)}{c^2} \left\{ \left(\frac{Gm}{r} + \dot{\phi}^2 r^2 - \dot{r}^2 \right) \sin 2W - 2r\dot{r}\dot{\phi} \cos 2W \right\}, \quad (14d)$$

$$P_0(l) = -\frac{S^2}{c^2} \left\{ \frac{Gm}{r} - \dot{\phi}^2 r^2 - \dot{r}^2 \right\}. \quad (14e)$$

Recall that the dynamical variables appearing in Eqs. (14) are parametrically given, in terms of u , by Eqs. (2) and (3), and require the solution to the 1PN accurate KE. The 2π -periodic functions $X_{2C}(l)$, $X_{2S}(l)$, $P_{2C}(l)$, $P_{2S}(l)$ and $P_0(l)$ allow Fourier series expansions that will be employed to obtain the spectral content of $h_{\times|Q}$ and $h_{+|Q}$. Let us first consider $H_{\times|Q}$. The fact that we can express $X_{2S}(l)$ and $X_{2C}(l)$ as

$$X_{2S}(l) = \sum_{j=-\infty}^{+\infty} S_j e^{ijl}, \quad (15a)$$

$$X_{2C}(l) = \sum_{j=-\infty}^{+\infty} C_j e^{ijl}, \quad (15b)$$

leads to

$$H_{\times|Q}(l) = \sum_{j=-\infty}^{+\infty} \bar{S}_j e^{i\omega_j^+ l} + \bar{C}_j e^{i\omega_j^- l}, \quad (16)$$

where

$$\bar{S}_j = \frac{e^{i2\phi_0}}{2} (C_j - iS_j), \quad (17a)$$

$$\bar{C}_j = \frac{e^{-i2\phi_0}}{2} (C_j + iS_j), \quad (17b)$$

$$\omega_j^+ = (j+2p), \quad \omega_j^- = (j-2p), \quad (17c)$$

$$p \equiv (1+k). \quad (17d)$$

Following Gopakumar & Iyer (2002), the Fourier series for $H_{\times|Q}$, relevant for computing its power spectrum, simplifies to

$$H_{\times|Q}^{\text{ps}} = \sqrt{2} \left\{ \sum_{j=1}^{\infty} (\bar{S}_j e^{i\omega_j^+ l} + \bar{C}_j e^{i\omega_j^- l}) + \bar{S}_0 e^{i2pl} \right\}, \quad (18)$$

where $H_{\times|Q}^{\text{ps}}$ denotes an expression required to compute the power spectrum of $H_{\times|Q}(l)$. In order to arrive at Eq. (18) from Eq. (16), we have used identities like $|\bar{S}_j|^2 = |\bar{C}_{-j}|^2$ and $|\bar{S}_{-j}|^2 = |\bar{C}_j|^2$. These relations are valid because ϕ_0 , X_{2C} and X_{2S} are real numbers. These inputs give us following expression to compute the ‘‘one-sided power spectrum’’ for $H_{\times|Q}$

$$H_{\times|Q}^{\text{ps}} = \sqrt{2} \left\{ \sum_{j=1}^{\infty} (\bar{S}_j e^{i(j+2p)l} + \bar{C}_j e^{i|j-2p|l}) + \bar{S}_0 e^{i2pl} \right\}, \quad (19)$$

From the above expression, we see that spectral lines appear at frequencies $(1+2p)f_r$, $(2+2p)f_r$, $(3+2p)f_r, \dots$ with strength $\sim |\bar{S}_1|^2, |\bar{S}_2|^2, |\bar{S}_3|^2, \dots$ respectively, where $f_r = n/2\pi$. Similarly, the ω_j^- part of Eq. (19) creates spectral lines at frequencies $|(1-2p)f_r|, |(2-2p)f_r, \dots$ with strength $\sim |\bar{C}_1|^2, |\bar{C}_2|^2, \dots$ respectively. Further, there will be an additional line at $2pf_r$ with strength $\sim |\bar{C}_0|^2 \equiv |\bar{S}_0|^2$.

Let us now sketch a similar analysis for $H_{+|Q}$ and its Fourier series expansion reads

$$H_{+|Q}(l) = \sum_{j=-\infty}^{+\infty} (\bar{S}_j^+ e^{i\omega_j^+ l} + \bar{C}_j^+ e^{i\omega_j^- l} + \bar{P}_j^0 e^{ijl}), \quad (20)$$

where \bar{S}_j^+ and \bar{C}_j^+ are defined in a manner similar to \bar{S}_j and \bar{C}_j , involving Fourier coefficients of P_{2S} and P_{2C} . In addition, \bar{P}_j^0 denote Fourier coefficients of $P_0(l)$. After following the details presented in Gopakumar & Iyer (2002), we obtain $H_{+|Q}^{\text{ps}}$, an expression required to compute the ‘‘one-sided power spectrum’’ for $H_{+|Q}$ as

$$H_{+|Q}^{\text{ps}} = \sqrt{2} \left\{ \sum_{j=1}^{\infty} (\bar{S}_j^+ e^{i(j+2p)l} + \bar{C}_j^+ e^{i|(j-2p)l}) + \bar{P}_j^0 e^{ijl} + \bar{C}_0^+ e^{i2pl} \right\} + \bar{P}_0^0. \quad (21)$$

It is important to note that in the case of $H_{+|Q}$ there exist spectral lines at $f_r, 2f_r, \dots$ that are unaffected by the advance of periastron parameter k . This follows from non- λ terms in $H_{+|Q}$.

It is now straightforward to compute the one-sided power spectrum for $H_{\times|Q}$ and $H_{+|Q}$ with the help of Eqs. (19) and (21). However, there are few technical details that need to be explained and let us, for simplicity, focus on $H_{\times|Q}$. It is clear from Eq. (19) that we require to evaluate C_j and S_j numerically. We employ Fast Fourier Transform routines from *Numerical Recipes* to evaluate C_j and S_j after obtaining $X_{2S}(l)$ and $X_{2C}(l)$. Recall that X_{2S} and X_{2C} ,

as given by Eqs. (14a) and (14b), are explicit functions of u and we use Mikkola's method, described in the previous section, to obtain $X_{2S}(l)$ and $X_{2C}(l)$ numerically. Further, we use the following exact relation for $v - u$ that appears in the expression for $W(u)$

$$v - u = 2 \tan^{-1} \left(\frac{\beta_\phi \sin u}{1 - \beta_\phi \cos u} \right), \quad (22)$$

where $\beta_\phi = \frac{1 - \sqrt{1 - e_\phi^2}}{e_\phi}$ [See Königsdörffer & Gopakumar (2006) for a detailed derivation of the above relation]. It is in the evaluation of $X_{2S}(l)$ and $X_{2C}(l)$ that we correct and improve shortcomings of a similar analysis done in Gopakumar & Iyer (2002). We observe that the PN accurate parametric expressions for r , \dot{r} and $\dot{\phi}$ appearing in Eqs. (14) were expanded into amplitude corrections to $h_{\times|Q}$ and $h_{+|Q}$ in Gopakumar & Iyer (2002) [see Eqs. (2.23) - (2.27) in Gopakumar & Iyer (2002)]. In this paper, we avoid this approach and treat r , \dot{r} and $\dot{\phi}$ in the same footing like $W(u)$ as done in Damour et al. (2004) and Königsdörffer & Gopakumar (2006). In Gopakumar & Iyer (2002), an inadequate approach was used to obtain $u(l)$ and further an approximate series expansion was employed for $v - u$ [see Eqs. (38) and (39) in Gopakumar & Iyer (2002)]. As explained earlier, we used a highly accurate and efficient method to compute $u(l)$ and an exact relation for $v - u$, given by Eq. (22), to obtain the time evolution of expressions appearing in Eqs. (14).

In order to make sure that the numerical codes that provided power spectra for $H_{\times|Q}$ and $H_{+|Q}$ do not contain bugs, we performed the following consistency check. We compared several temporal plots for $H_{\times|Q}(l)$, created with the help of Eq. (16), with those originating from the procedure detailed in Section 2 and 3, which does not require the evaluation of various Fourier coefficients. For any given orbital configuration, we found excellent agreement between these two temporal plots, created with two distinct procedures. A similar analysis was also performed for $H_{+|Q}(l)$.

We note that Eqs. (16) and (20), representing Fourier series of $H_{\times|Q}(l)$ and $H_{+|Q}(l)$, are the starting points to investigate the data analysis issues, associated with $h_{\times|Q}(t)$ and $h_{+|Q}(t)$. This is because the signal received at LISA will have induced amplitude, frequency and phase modulations on $h_{\times|Q}(t)$ and $h_{+|Q}(t)$, as detailed in Cutler (1998) and Rogan & Bose (2006). It is convenient to incorporate these modulations using Eqs. (16) and (20) rather than using Eqs. (1). This is one of the reasons for explaining in detail how we compute Fourier domain versions of Eqs. (1).

In the next section, we present our results and explain their salient features.

5 DISCUSSIONS

Let us begin by presenting several plots that depict our computations. In Figs. 1 and 2, we present scaled $h_{\times|Q}(l)$ and $h_{+|Q}(l)$ ($H_{\times|Q}(l)$ and $H_{+|Q}(l)$) for stellar-mass compact binaries ($m_1 = m_2 = 1.4 M_\odot$) for various eccentricities when $n \sim 6.28 \times 10^{-3} \text{ Hz}$ and $i = \pi/3$. The associated normalized power spectrum is also displayed in Figs. 3 and 4. We clearly see, as expected, as we increase the value of e_t , higher harmonics with appreciable strengths appear and the total

power gets distributed among several frequencies. The burst nature of the GW signal at high eccentricities indicates the strong emission of gravitational waves near the periastron due to higher relative velocity around the periastron. Another point to note is that spectral lines are all apparently at multiples of radial orbital frequency f_r and we do not observe the effect of periastron advance in Figs. 3 and 4. Recall that the periastron advance causes splitting and shifting of spectral lines compared to the Newtonian case. However, in our cases, the shifting of lines from their (Newtonian) positions is too small to be visible in our graphs. The dimensionless parameter k , characterizing the periastron advance, is $\sim 5.9 \times 10^{-5}$ for $e_t = 0.1$ and $\sim 3.1 \times 10^{-4}$ for $e_t = 0.9$ [For $n \sim 6.28 \times 10^{-3} \text{ Hz}$ and $m = 2.8 M_\odot$]. The frequency shift caused by k , deducible from the previous section, is $2k f_r$ and in the case of our stellar-mass binaries this is $\sim 1.2 \times 10^{-7} \text{ Hz}$ for $e_t = 0.1$ and $\sim 6.2 \times 10^{-7} \text{ Hz}$ for $e_t = 0.9$. Therefore, it is reasonable to expect that one year LISA observation, which can lead to frequency resolution $\sim 3 \times 10^{-8} \text{ Hz}$, should be sensitive to k and hence its effect cannot be neglected in the search templates. It is also straightforward in our prescription to drop the effect of k , which can be achieved by neglecting 1PN corrections to the orbital dynamics given in Section 2. We display Table 1 to show that the periastron advance creates closely spaced triplets of spectral lines, corresponding to different values of j , which are not visible in Figs. 3 and 6. Though triplets are created, one of them really dominates the other two in strength. Further, the dominant one always corresponds to the lowest possible j value for that particular triplet. In another set of plots (Figs. 5 and 6), we examine the effect of orbital inclination on $H_{+|Q}$ and its normalized power spectrum. We observe that the influence of i is more visible in the temporal evolution rather than in the associated frequency spectrum. We do not display similar plots for $H_{\times|Q}$ as its simple dependence on i , defined by $\cos i$, is clearly visible in Eq. (1). We also investigated if the ratio of the relative power spectrum of $H_{+|Q}$ and $H_{\times|Q}$ can be used to obtain information about the orbital inclination. From Fig. 7 we infer that the above mentioned ratio is rather independent of eccentricity and can be used to estimate the value of i .

Let us now discuss why our prescription to compute $h_{\times|Q}$ and $h_{+|Q}$ is superior to what is available in the literature (Moreno-Garrido et al. 1995, Pierro et al. 2001). In Moreno-Garrido et al. (1995), though the orbital motion is Newtonian accurate, the effect of periastron advance was introduced by hand. This was achieved by imposing that the periastron advance causes the relative position of the observer to change in a uniform manner with respect to the semi-major axis of the orbit. This leads to certain ad-hoc splitting and shifting of the spectral lines. Further, the effect of periastron advance and the Newtonian accurate orbital dynamics, available in Moreno-Garrido et al. (1995), do not require to specify the individual masses m_1 and m_2 , but only the total mass m . However, our fully 1PN accurate orbital description demands m and η and hence the specification of m_1 and m_2 . Pierro et al. (2001), while neglecting the imposed effect that mimics the true periastron advance, employed Newtonian accurate orbital motion and an approximate analytic expression for the Bessel functions required to compute the infinite series appearing in the temporal evolution for $h_{\times|Q}$ and $h_{+|Q}$. Recall that $J_n(ne)$ and $J'_n(ne)$,

Bessel functions of the first kind and their first derivatives, available in Moreno-Garrido et al. (1995) and Pierro et al. (2001), arise from the Fourier analysis of the classical (Newtonian accurate) Keplerian motion.

While comparing our computations with those presented in Moreno-Garrido et al. (1995) and Pierro et al. (2001), we realized that Eqs. (13) of Moreno-Garrido et al. (1995) give correct circular limit (Blanchet et al. 1996) for $h_{\times|Q}$ and $h_{+|Q}$. However, Eqs.(6) and (7) of Pierro et al. (2001) differ, in the circular limit, from Eqs. (2), (3a) and (4a) of Blanchet et al. (1996) by a factor of $-\sqrt{2}$. The difference in sign may be associated with the usage of a different set of conventions compared to the one used here and in Blanchet et al. (1996). However, this is not desirable because for the data analysis purposes, $h_{\times|Q}$ and $h_{+|Q}$ need to be combined with F_{\times} and F_{+} , the so-called beam-pattern functions of the GW detector (Thorne 1987). The convention, *i.e.*, the way of prescribing a triad that specifies the direction and orientation of the binary orbit, is chosen in Blanchet et al. (1996) and here such that the resulting $h_{\times|Q}$ and $h_{+|Q}$ can be directly combined with expressions for F_{\times} and F_{+} , available in Thorne (1987).

However, as our approach is semi-numerical, almost analytic investigations of Moreno-Garrido et al. (1995) and Pierro et al. (2001) can be used to check our results, especially for small eccentricities. We restricted comparisons of our results with those of Moreno-Garrido et al. (1995) and Pierro et al. (2001) to moderate eccentricities as it is rather difficult and time consuming to compute accurately large number of $J_n(ne)$ and $J'_n(ne)$, required for high eccentricities. We find good qualitative agreement with plots available in Moreno-Garrido et al. (1995) and Pierro et al. (2001). Finally, we note that our approach is quite close to the way Wahlquist obtained $h_{\times|Q}(t)$ and $h_{+|Q}(t)$, with Newtonian accurate orbital motion, in the context of spacecraft Doppler detection of gravitational waves from widely separated massive black holes (Wahlquist 1987). It is interesting to note that the KE is expressed in terms of v rather than u in Wahlquist (1987) and hence inversed trigonometric functions appear in the classical KE [It is quite subtle to solve the KE expressed in terms of v]. As expected, our waveforms with Newtonian accurate orbital motion, are in excellent agreement with those given in Wahlquist (1987).

We, therefore, conclude that our fully 1PN accurate prescriptions to compute temporal evolutions for $h_{\times|Q}$ and $h_{+|Q}$ and their associated power spectra, which do not require the infinite series expansions whose coefficients contain $J_n(ne)$ and $J'_n(ne)$, are always going to be more accurate and computationally efficient compared to those currently available in the literature.

A rough indicator for the applicability of our waveforms can be obtained by comparing LISA's frequency resolution for one year, $\Delta f_{LISA} \sim 3 \times 10^{-8} \text{Hz}$, with the frequency shifts caused by the advance of periastron and radiation reaction. The frequency shift of any harmonic due to the periastron advance, as explained earlier, reads

$$\Delta f_k \sim \frac{1.2 \times 10^{-7}}{(1 - e_t^2)} \left(\frac{m}{2.8 M_{\odot}} \right)^{2/3} \left(\frac{f_r}{10^{-3} \text{Hz}} \right)^{5/3} \text{Hz}. \quad (23)$$

The radiation reaction also causes a secular drift in f_r and

this drift in one year is

$$\Delta f_{RR} \sim \frac{1.6 \times 10^{-9}}{(1 - e_t^2)^{7/2}} \left(\frac{m}{2.8 M_{\odot}} \right)^{5/3} \left(\frac{\eta}{0.25} \right) \left(\frac{f_r}{10^{-3} \text{Hz}} \right)^{11/3} \times \left(1 + \frac{73}{24} e_t^2 + \frac{37}{96} e_t^4 \right) \text{Hz}. \quad (24)$$

The above expression is obtained by computing the change in f_r using the leading order orbital averaged contributions to dn/dt from Damour et al. (2004). The rough limits on the applicability of our waveforms are provided by investigating if LISA can resolve the above two frequency shifts.

We provide rough limits on the applicability of our $h_{\times,+|Q}(l)$ by considering three binary configurations. Let us first consider the case, where $m_1 = m_2 \sim 1.4 M_{\odot}$, $e_t = 0.9$ and $f_r \sim 10^{-4} \text{Hz}$. For this binary, $\Delta f_k \sim 1.3 \times 10^{-8} \text{Hz}$ and $\Delta f_{RR} \sim 4 \times 10^{-10} \text{Hz}$ indicating that Newtonian accurate orbital description will be sufficient as $\Delta f_{LISA} > \Delta f_k$ and $\Delta f_{LISA} \gg \Delta f_{RR}$. For NS-NS binaries, with $f_r \sim 10^{-3} \text{Hz}$, $e_t \sim 0.5$, $\Delta f_k \sim 1.5 \times 10^{-7} \text{Hz}$ and $\Delta f_{RR} \sim 7.5 \times 10^{-9} \text{Hz}$ indicating that our $h_{\times,+|Q}(l)$ with 1PN accurate orbital dynamics will be important to detect these binaries. We do not recommend the use of ad hoc gravitational waveforms, available in Moreno-Garrido et al. (1995), as these $h_{\times,+|Q}$ will not provide any information about η and are not computationally efficient as explained earlier. A rough upper limit of applicability is provided by BH-NS binaries with $m \sim 10 M_{\odot}$, $e_t \sim 0.2$ and $f_r \sim 10^{-3} \text{Hz}$. This is because for such binaries $2 \times \Delta f_{RR} \sim \Delta f_{LISA}$ (1 year) and therefore, it is important to have $h_{\times,+|Q}$ that include effects of gravitational radiation reaction. While treating extremely eccentric binaries at 1PN order, care should be taken so that e_{ϕ} does not exceed unity. This is also a limit of applicability of our $h_{\times,+|Q}(l)$ with 1PN accurate orbital motion.

It should be noted that in all the cases above we assumed that the emitted gravitational waves, in some cases at higher harmonics, are sufficiently strong in amplitudes to be observed by LISA. A realistic investigation about the advantage and applicability of our $h_{\times,+|Q}(l)$ is currently under investigation in Bose et al. (2006).

6 CONCLUSIONS

We provided an accurate and computationally efficient prescription to obtain GW polarizations associated with non-spinning bound compact binaries of arbitrary eccentricity and mass ratio, moving in slowly precessing orbits. In PN description, we restricted the orbital motion to be 1PN accurate and considered only quadrupole contributions to the amplitudes of h_{\times} and h_{+} . We employed an accurate (numerical) method due to Mikkola to solve the relevant KE appearing in our orbital description. The time domain $h_{\times|Q}$, $h_{+|Q}$ and their associated frequency spectrum, provided in this paper, should be required by LISA to detect and analyze gravitational waves from stellar-mass detached compact binaries moving in eccentric and precessing orbits. Therefore, we expect that our accurate and efficient prescription to compute $h_{\times|Q}$ and $h_{+|Q}$ should be of definite interest to the recently initiated *mock LISA data challenge* task force. It is possible to extend our prescription to include effects due to radiation reaction (Damour et al. 2004; Königsdörffer & Gopakumar 2006), spin-orbit interactions

(Königsdörffer & Gopakumar 2006) and amplitude corrections. Many of these projects are currently in progress.

ACKNOWLEDGMENTS

We are grateful to Gerhard Schäfer and Seppo Mikkola for discussions and encouragements. It is our pleasure to thank Sukanta Bose, Bala Iyer, and Christian Königsdörffer for carefully reading the manuscript and for useful comments. This work is supported by the Deutsche Forschungsgemeinschaft (DFG) through SFB/TR7 “Gravitationswellenastronomie”.

REFERENCES

- Benacquista M. J., 2002, *Class. Quant. Grav.*, 19, 1297.
Blanchet L., Iyer B. R., Will C. M., Wiseman A. G., 1996, *Class. Quant. Grav.*, 13, 575
Bose S., Gopakumar A., Rogan A., 2006, work in progress.
Rogan A., Bose S., 2006, astro-ph/0605034
Chaurasia H. K., Bailes M., 2005, *ApJ*, 632, 1054
Colwell P., *Solving Kepler’s Equation Over Three Centuries* (Willman-Bell, Inc., Richmond, 1993)
Cutler C., 1998, *Phys. Rev. D*, 57, 7089-7102
Damour T., Deruelle N., 1985, *Phys. Theor.*, 43, 107
Damour T., Gopakumar A., Iyer B. R., 2004, *Phys. Rev. D*, 70, 064028
Danby J. M. A., Burkardt T. M., 1983, *Celestial Mechanics*, 31, 95 - 107
Gopakumar A., Iyer B. R., 2002, *Phys. Rev. D* 65, 084011
Gusev A.V., Ignatiev V.B., Kuranov A.G., Postnov K.A., Prokhorov M.E., 2002, *Astron. Lett.* 28, 143-149 (astro-ph/0111066)
Jones D. I., 2005, *ApJ*, 618, L115
Königsdörffer C., Gopakumar A., 2005, *Phys. Rev. D* 71, 024039
Königsdörffer C., Gopakumar A., 2006, *Phys. Rev. D* 73, 124012
Mikkola S., 1987, *Celestial Mechanics*, 40, 329 - 334
Moreno-Garrido C., Mediavilla E., Buitrago J., 1995, *MNRAS*, 274, 115
Pierro V., Pinto, I. M., Spallicci A. D., Laserra E., Recano F., 2001, *MNRAS*, 325, 358
Seto N., 2001, *Phys. Rev. Lett.*, 87, 251101
Thorne K. S., *300 Years of Gravitation*, edited by Hawking S. W. and Israel W. (Cambridge University Press, Cambridge, 1987), p. 330.
Wahlquist H., 1987, *Gen. Relativ. Gravitation*, 19, 1101

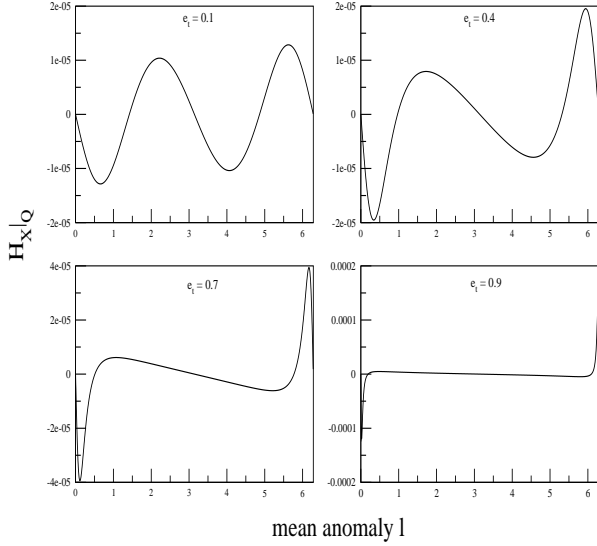


Figure 1. Time domain plots of $H_{\times}|_Q(l)$ for various eccentricities. The other orbital parameters are $m_1 = m_2 = 1.4M_{\odot}$, $i = \pi/3$ and $n = 6.28 \times 10^{-3}\text{Hz}$.

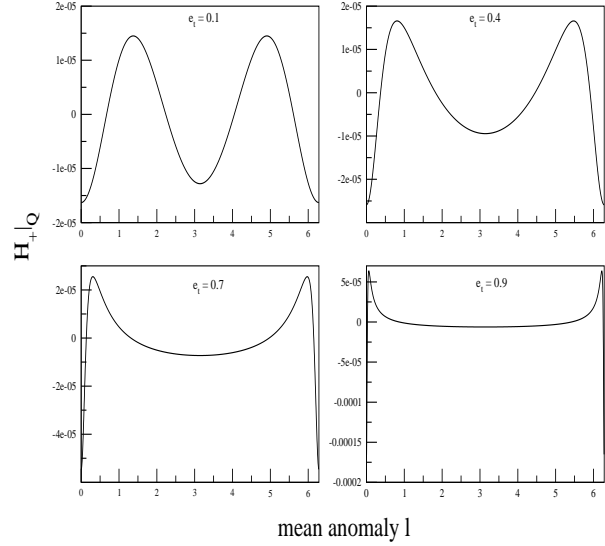


Figure 2. Plots, similar to Fig. 1, for $H_{+}|_Q(l)$.

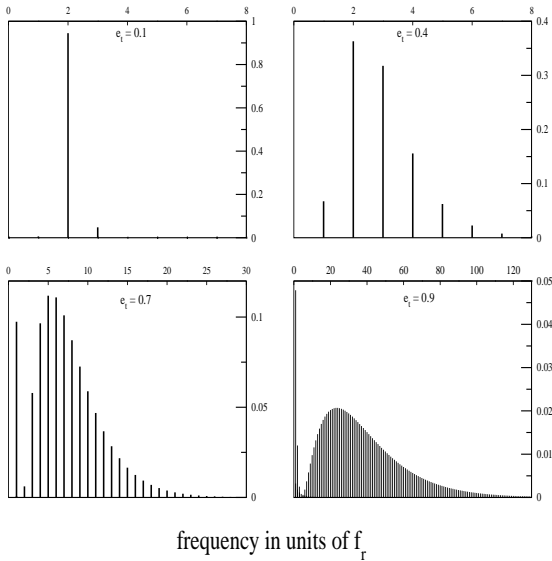


Figure 3. The normalized relative power spectrum plotted against the frequency in units of f_r associated with $H_{\times}|_Q$ displayed in Fig. 1. As eccentricity increases, the dominant harmonic shifts its position, and the total power gets distributed among the higher ‘harmonics’.

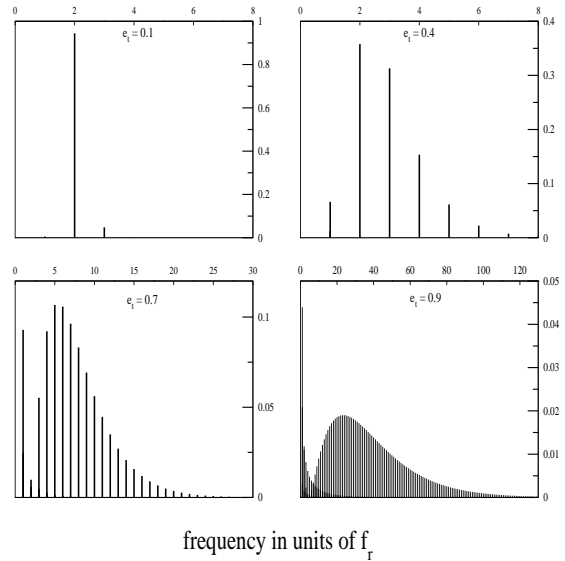


Figure 4. The normalized relative power spectrum associated with various $H_{+}|_Q$ plots displayed in Fig. 2.

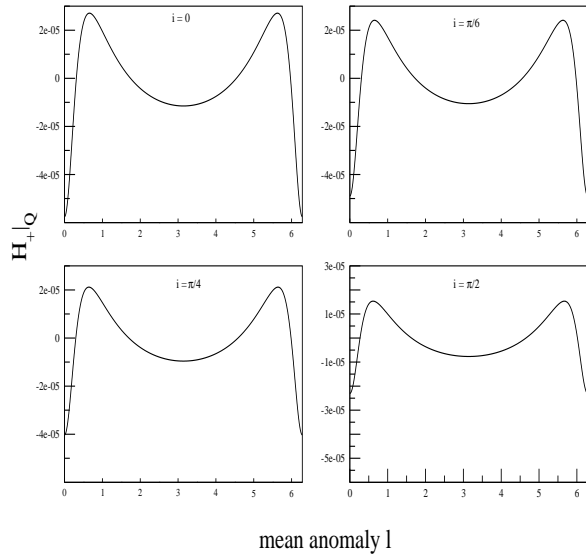


Figure 5. Plots for $H_+|_Q$ that explore its dependence on the orbital inclination. We used the following orbital parameters: $m_1 = m_2 = 1.4M_\odot$, $e_t = 0.5$ and $n \sim 10^{-3}$ Hz.

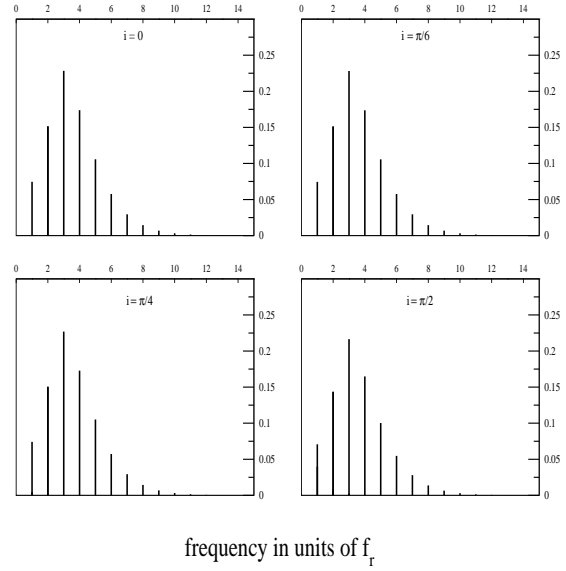


Figure 6. Plots of the normalized power spectrum for various values of i associated with Fig. 5. The dependence on i is rather difficult in perceive.

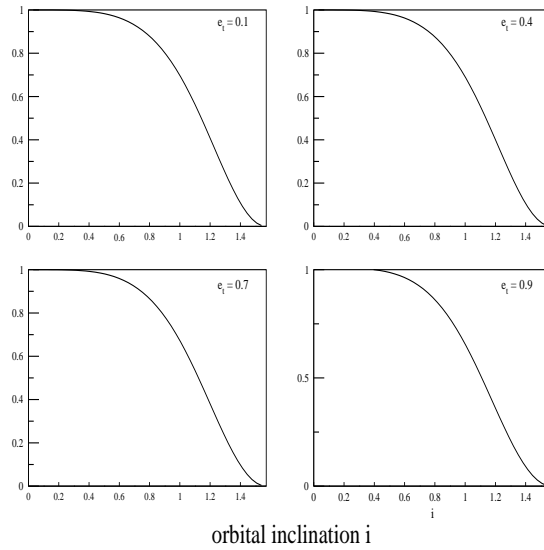


Figure 7. Plots that depict the ratio of the total power present in $H_\times|_Q$ and $H_+|_Q$ as functions of the orbital inclination for various eccentricities. The ratio is independent of eccentricity and hence can be used to bound i .

Table 1. Spectral lines associated with $H_+|Q$, and with normalized strengths, appearing at several frequencies (in units of f_r) for various e_t . We let $m_1 = m_2 = 1.4 M_\odot$, $n \sim 6.28 \times 10^{-3}$ Hz, and $i = \pi/3$. Though the summation index j , appearing in Eq. (21), takes integer values, spectral lines appear at $|j - 2p|$, j and $|j + 2p|$. We note that different values of j contribute to a closely spaced triplet and one of these lines dominates, in its strength, the other two. We observed that normalized value for \bar{P}_0^0 is always negligible.

	$e_t = 0.1$		$e_t = 0.3$		$e_t = 0.5$			
	frequency in units of f_r		frequency in units of f_r		frequency in units of f_r			
$j = 0$	2.00012	0.94409	$j = 0$	2.00013	0.57851	$j = 0$	2.00016	0.17427
	0.00000	~ 0		0.00000	~ 0		0.00000	~ 0
$j = 1$	1.00012	0.00553	$j = 1$	1.00013	0.04285	$j = 1$	1.00016	0.08588
	1.00000	0.00089		1.00000	0.00742		1.00000	0.01733
	3.00012	0.04793		3.00013	0.27243		3.00016	0.26293
$j = 2$	0.00012	~ 0	$j = 2$	0.00013	~ 0	$j = 2$	0.00016	~ 0
	2.00000	0.00001		2.00000	0.00064		2.00000	0.00390
	4.00012	0.00151		4.00013	0.07596		4.00016	0.20020
$j = 3$	0.99988	~ 0	$j = 3$	0.99987	~ 0	$j = 3$	0.99984	0.00009
	3.00000	~ 0		3.00000	0.00007		3.00000	0.00110
	5.00012	0.00004		5.00013	0.01753		5.00016	0.12183
$j = 4$	1.99988	~ 0	$j = 4$	1.99987	~ 0	$j = 4$	1.99984	0.00002
	4.00000	~ 0		4.00000	0.00001		4.00000	0.00034
	6.00012	~ 0		6.00013	0.00367		6.00016	0.06647
$j = 5$	2.99988	~ 0	$j = 5$	2.99987	~ 0	$j = 5$	2.99984	~ 0
	5.00000	~ 0		5.00000	~ 0		5.00000	0.00011
	7.00012	~ 0		7.00013	0.00073		7.00016	0.03401